EMISSION TRIGGERING IN THE MAGNETOSPHERE BY CONTROLLED INTERRUPTION OF COHERENT VLF SIGNALS

D. C. D. Chang[1] and R. A. Helliwell

Radioscience Laboratory, Stanford University, Stanford, California 94305

Abstract. Man-made VLF whistler mode (WM) waves are employed in controlled experiments on wave growth and triggering within the magnetosphere. In one such experiment, VLF pulses of 1-s duration are interrupted by a 10-ms gap. Two types of gap are employed. In the first, the phase of the wave following the gap is the same as that of a constant-frequency wave with no gap. In the second type, this phase is reversed. The data indicate that the growth rate and saturation level of the postgap section of a pulse are independent of the phase shift introduced in the gap. Moreover, it is often observed that rising frequency emissions are triggered during the 10-ms gap. They closely resemble those emissions that frequently appear near the ends of constant-frequency signals. The gap-induced emissions may then interact with the postgap signals. Suppressions and entrainments between those signals are often observed. An explanation of the phenomenon of gap-induced emissions is based on the hypothesis that the radiation from the wave-organized electrons can switch from a 'forced' mode to a 'natural' mode after termination of the triggering wave. An experiment on the relation between gap length and the development of falling emissions confirms an earlier observation that falling emissions always start with a small rise in frequency. It also shows that a postgap signal can 'capture' a gap-induced falling emission when its frequency is close to that of the postgap signal at its beginning.

Introduction

Recently, many experiments have been performed on VLF wave-particle interaction (WPI) processes by injecting controlled VLF waves into the magnetosphere from Siple Station, Antarctica [Helliwell and Katsufrakis, 1974; Helliwell et al., 1975; Raghuram et al., 1977a, b; Stiles and Helliwell, 1977]. The output signals are detected at the Siple conjugate point near Roberval, Canada. Similar wave injection experiments have been conducted between Alaska and New Zealand [McPherson et al., 1974; Koons et al., 1976; Dowden et al., 1978].

The amplified waves and triggered emissions may dump electrons into the ionosphere, exciting X-rays [Rosenberg et al., 1971], perturbing the electron density sufficiently to affect subionospheric VLF propagation [Helliwell et al., 1973], and modulating the local conductivity, which may in turn excite ULF waves [Bell, 1976]. It is important therefore to understand the mechanisms that govern the growth and generation of coherent VLF waves in the magnetosphere.

It has been suggested that coherent wave amplification is the result of phase-bunched electrons [Brice, 1964; Helliwell, 1967; Helliwell and Crystal, 1973; Nunn, 1974]. The whistler mode waves phase-bunch the counter-streaming electrons in the so-called interaction region, where the electrons are approximately in resonance with the wave. These phase-bunched electrons constitute transverse currents that cause the waves to grow. In this paper we present results from new experiments designed to show how changes in the phase and continuity of the transmitted wave affect wave growth and emission triggering. Because of inherent limitations of the transmitter employed in these experiments, a phase alteration in the applied VLF signal requires the insertion of a 10-ms pulse that is offset in frequency from the main signal by several hundred hertz. The frequency offset is made so large (~300 Hz) that the 10-ms pulse does not interact significantly with the electrons in resonance with the main signal. The applied signal can therefore be viewed as having been interrupted by a 10-ms gap. The portion of the signal following the gap is either in or out of phase with that preceding the gap.

The data show that the postgap growth rates and the saturation levels of the main signals are independent of the postgap phase. Furthermore, a rising emission often is induced by a 10-ms gap. These gap-induced emissions may develop into fully independent rising emissions, or they may be either suppressed or entrained by the applied signal. When the gap length exceeds 70 ms, there may appear a fully developed falling tone emission that begins with a slight rise in frequency. It closely resembles the 'tail-end' emissions seen at the ends of many constant frequency pulses. At smaller gap lengths the falling tone is captured by the returning applied pulse. At 70 ms, capture also occurs but is accompanied by an overshoot of roughly 100 Hz below the applied signal.

To explain the phenomenon of gap-induced emissions, it is suggested that the radiation from the wave-organized electrons switches from its forced mode to its natural mode at the end of the applied wave [Helliwell, 1978]. In the forced mode all currents are in the steady state and all radiation components have the frequency of the driving wave. When the drive is removed, the existing currents cannot decay instantaneously but radiate over a range of frequencies determined by their 'natural' modes. The detailed mechanism of the development of the gap-induced emissions is under study and will be reported in a later paper.

[1]Presently with Hughes Aircraft Company, Space and Communications Group, El Segundo, Calif.

Paper number 9A1349.
0148-0227/79/009A-1349$01.00

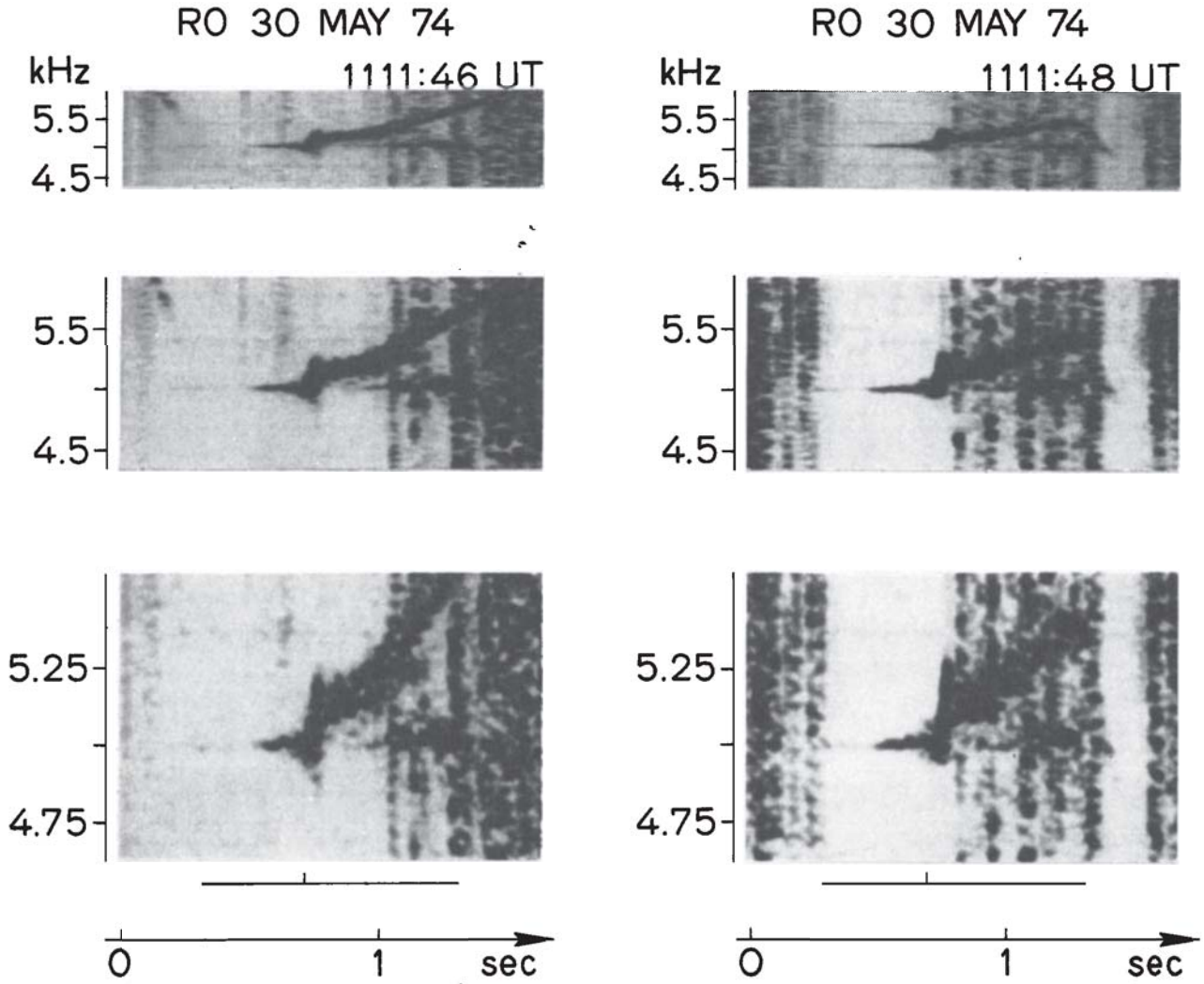

Figure 1. Two examples of typical gap-induced emissions. The middle and the lower panels contain the same data as that in the upper panel but are expanded in the frequency scale by factors of 2 and 5, respectively. Both of the 1-s triggering signals at 5 kHz are interrupted by a 10-ms gap after 400 ms. The duration of the signals is indicated beneath the lower panel by the horizontal bars on which the small vertical bars indicate the time of interruptions. A rising emission with df/dt ~ 8 kHz/s is induced by each interruption. The emissions appear to feed energy to the eighty-fifth and the eighty-sixth PLH at 5.1 and 5.16 kHz, respectively, which in turn induce rising emissions with df/dt ~ 1 kHz/s.

The remaining section of this paper describes the results of several fixed- and variable-gap experiments.

Gap-Triggering Experiments

To explore the phase-bunching concept, an experiment was performed to determine how the growth rate and the saturation level of a wave would be affected simply by reversing the phase of the triggering wave. It was thought that a phase reversal would tend to debunch the electrons and hence reduce growth.

As was mentioned earlier, a phase shift is produced by shifting the carrier frequency by a few hundred hertz for a period of 10 ms, creating in effect a 10-ms gap in the main signal. The amount of this phase change is given by

$$\Delta\phi = 2\pi\Delta f\Delta t \qquad (1)$$

where Δt = 10 ms. Setting Δf to ±350 Hz gives a phase shift of $\pm 6\pi$ (in phase) and $\pm 7\pi$ (in antiphase), respectively. For simplicity we denote the in-phase condition by 0 and the antiphase condition by π.

At the time the experiment was designed it was assumed that the 10-ms gap would be too short to affect the wave growth processes and that the main effect would come from the phase reversal. The data show that in fact the main effect comes from the gap and not the phase shift. The growth rates and the saturation levels of the signals after the interruptions are the same regardless of whether the triggering wave is a π wave or an 0 wave. In addition, rising frequency emissions often are induced by the gaps. These gap-induced emissions may de-

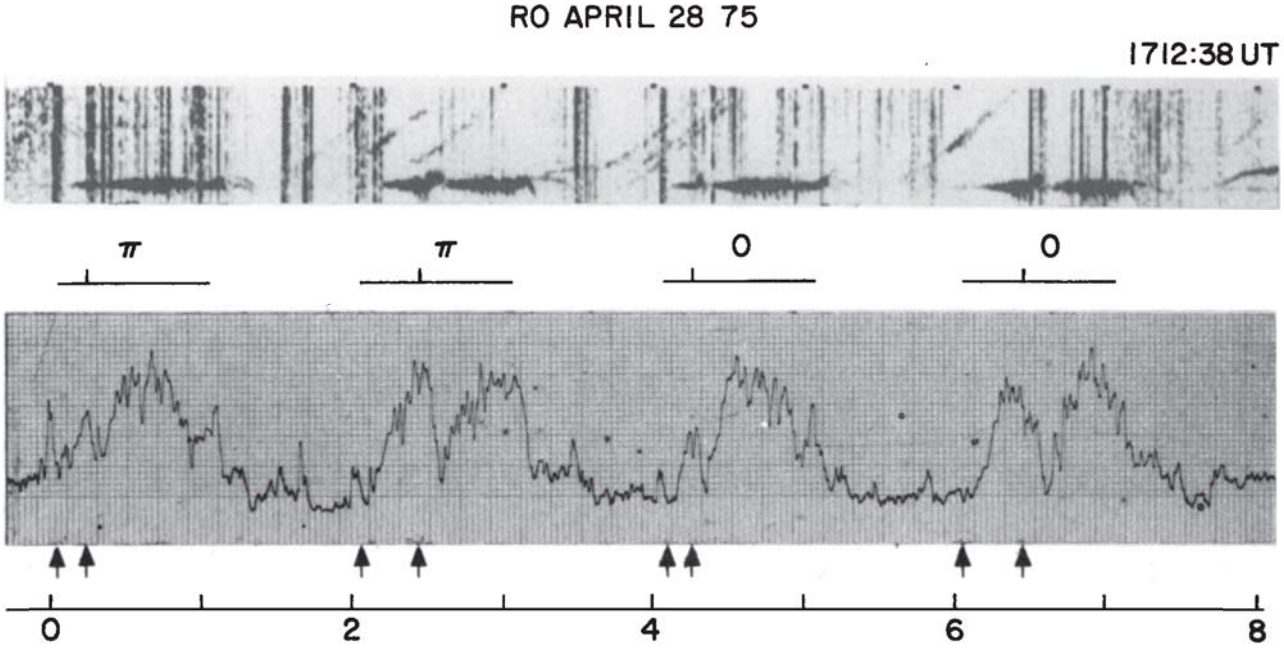

Figure 2. Examples of gap-induced emissions. Upper panel shows the dynamic spectrum. Lower panel shows amplitude (log scale) measured in a 340-Hz band centered at 4.5 kHz. The interruptions occur at the two-hundredth or four-hundredth millisecond as indicated by the vertical bars in the middle panel. Shortly after each gap the amplitude drops approximately to the noise level and then grows again. The initial and postgap growth rates are almost identical regardless of whether the triggering wave is in the 0 or a π condition. The saturation level is also independent of the 0 or π condition. The growth time is about 250 ms.

velop into fully independent rising emissions, or be suppressed or entrained by the applied signals.

The actual length of the gap at the equatorial plane, where the interaction is assumed to occur, may be increased significantly by frequency dispersion. This effect increases as the frequency departs from the nose frequency on the path. For example, a zero-gap phase reversal creates a 10-ms gap at the equator for f = 6.6 kHz, L = 3.1, and an equatorial density of 1000/cc [Chang, 1978].

The applied signals are both π waves at 5 kHz. Both last for 1 sec and are interrupted at the four hundredth ms by a 10-ms gap. The duration of the applied signal is indicated by the 1-sec-long horizontal bar just above each time scale. The times of interruptions are indicated by the small vertical bars. The delay time of the gap with respect to the beginning of the signal is called τ_d.

There were several ducts in the magnetosphere in this period as evidenced by the multiple traces of whistlers on the Roberval data (not shown). (Unfortunately, in experiments of this type it is seldom possible to obtain data that are completely free of multipath effects.) Only two whistler traces were observable above 4.8 kHz. The corresponding measured two-hop delays were ~2.10 and ~2.62 s at 5 kHz. Moreover, the second whistler was much stronger than the first. (The L values of these ducts were found by a standard curve-fitting method [Smith and Carpenter, 1961; Ho and Bernard, 1973] to be 3.3 and 3.5, respectively.)

The one-hop delay of the observed signals (measured at the gaps and the ends of the pulses) was ~1.3 s, in good agreement with the delay time of the second whistler (at L ~3.5). Therefore we conclude that the observed signals can be viewed as having traveled on a single path at L = 3.5.

In Figure 1 the first example (1111:46 UT) shows that a rising emission is developed near the time of the 10-ms gap. The slope of the gap-induced emission is about 8 kHz/s. As the emission develops it appears to feed energy to the eighty-fifth and eighty-sixth power line harmonics (PLH) at 5.10 and 5.16 kHz, respectively. (The PLH are believed to be signals radiated by the North American power distribution systems [Helliwell et al., 1975].) The PLH then trigger emissions with df/dt ≈ 1 kHz/s. The gap-induced emission with df/dt ≈ 8 kHz/s is quenched near 5.25 kHz. Because of dispersion from the equatorial plane (assumed location of source) to the ground, the corresponding values of df/dt in the interaction region will be somewhat less because all frequencies of the emission are below the nose frequency. By using standard methods the actual value of df/dt at the location of generation is estimated to be 6 kHz/s.

The second example (1111:46 UT) shows almost the same features of gap-induced emissions as the first. The gap-induced emission again has a slope of df/dt ≈ 8 kHz/s and is quenched near 5.3 kHz. However, the upper PLH emission, at 5.16 kHz, is not as well-defined as in the first example.

In both examples the applied signal suddenly decreases in magnitude at the time of triggering. As the emission rises in frequency the applied signal starts to grow again. It reaches

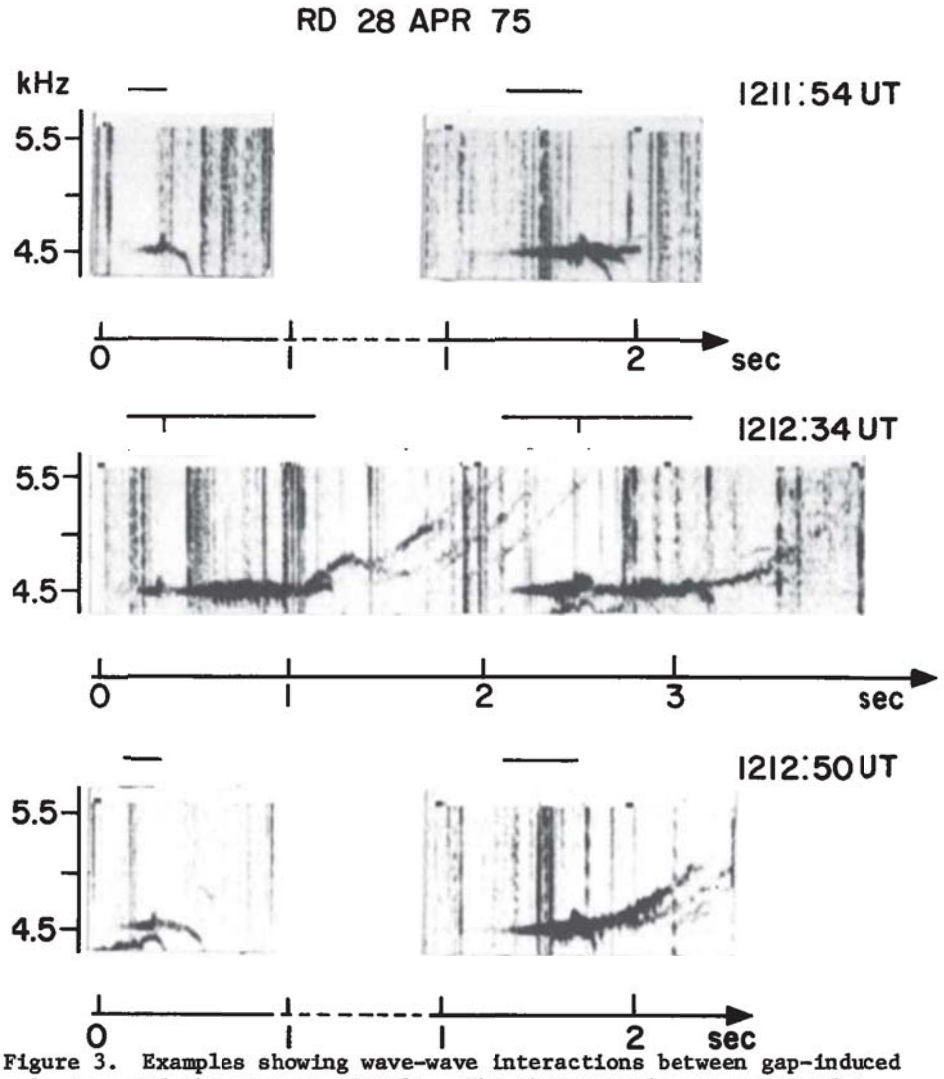

Figure 3. Examples showing wave-wave interactions between gap-induced emissions and the postgap signals. The three panels are arranged in chronological order. The calibration waves, shown in the upper and the lower panels, are 200- and 400-ms constant-frequency signals. As is indicated by the horizontal bars on the tops of the panels, these signals have exactly the same durations as the pregap sections of the gap-triggering waves on the middle panel. The calibration waves trigger BLI-type emissions followed by falling and/or rising tone emissions, while the pregap sections of the gap-triggering signals induce only BLI-type emissions. No falling or rising emissions are observed following BLIs, indicating that the emissions are either suppressed or entrained by the postgap section of the main panel.

the threshold of detection about 200 ms after the gap, which is the same as for the initial signal.

The amplitude behavior of the applied signal before and after the gap is illustrated by four more examples, shown in Figure 2. Here, τ_d is 200 or 400 ms, as indicated in the middle panel by a vertical bar below the '0' or 'π' symbol.

Analysis of whistlers showed that several paths were active at the time, with one dominant path at L ~ 4.6.

The signal amplitude measured with a narrowband filter (340 kHz) centered at 4.5 kHz shows an initial growth rate of 75 ± 10 dB/s in all four examples and a growth time of roughly 250 ms. (Growth time is defined as the time period required for the signal to grow to 80% of its peak value.) It is seen that when τ_d = 200 ms, the gap occurs before saturation, while for τ_d = 400 ms, the gap occurs after saturation. Associated with the gaps are very pronounced amplitude drops in the main signals. (A similar effect has been seen in periodic emission triggering by a key-down signal [Helliwell and Katsufrakis, 1974].) The growth rate and saturation level are the same as before the gap (within observational error), regardless of whether the signal is 0 or π.

The spectrogram in the upper panel of Figure 2 shows that the emissions triggered in the gaps are not fully developed. Two possible causes are suppression or entrainment by the main signal.

The nature of the postgap behavior is demon-

TABLE 1. Averaged Initial Growth Rate, Postgap Growth Rate, and Saturation Level Over 52 Examples Taken on April 28 and May 13, 1975, for Both 0 Waves and π Waves

τ_d	200 ms		400 ms		Average
Wave type	0	π	0	π	
Initial growth rate, dB/s	79 (26)*	79 (23)	76 (27)	78 (23)	78
Growth rate after gap, dB/s	74 (27)	78 (26)	74 (30)	77 (23)	76
Saturation† level, dB	15 (2.8)	14 (3.3)	16 (2.8)	16 (3.2)	15

*(M) indicates the standard deviation.

†Above noise level.

strated by a related experiment in which the sequences of Figure 2 are compared with simple pulses of duration 200 or 400 ms. The results are shown in Figure 3, where the 200- and 400-ms pulses observed just before and after the gap pulses of the middle panel are displayed in the upper and lower panels, respectively.

It is clear that both the 200- and 400-ms pulses trigger emissions of the 'band-limited impulse' (BLI) type [Helliwell, 1978], followed

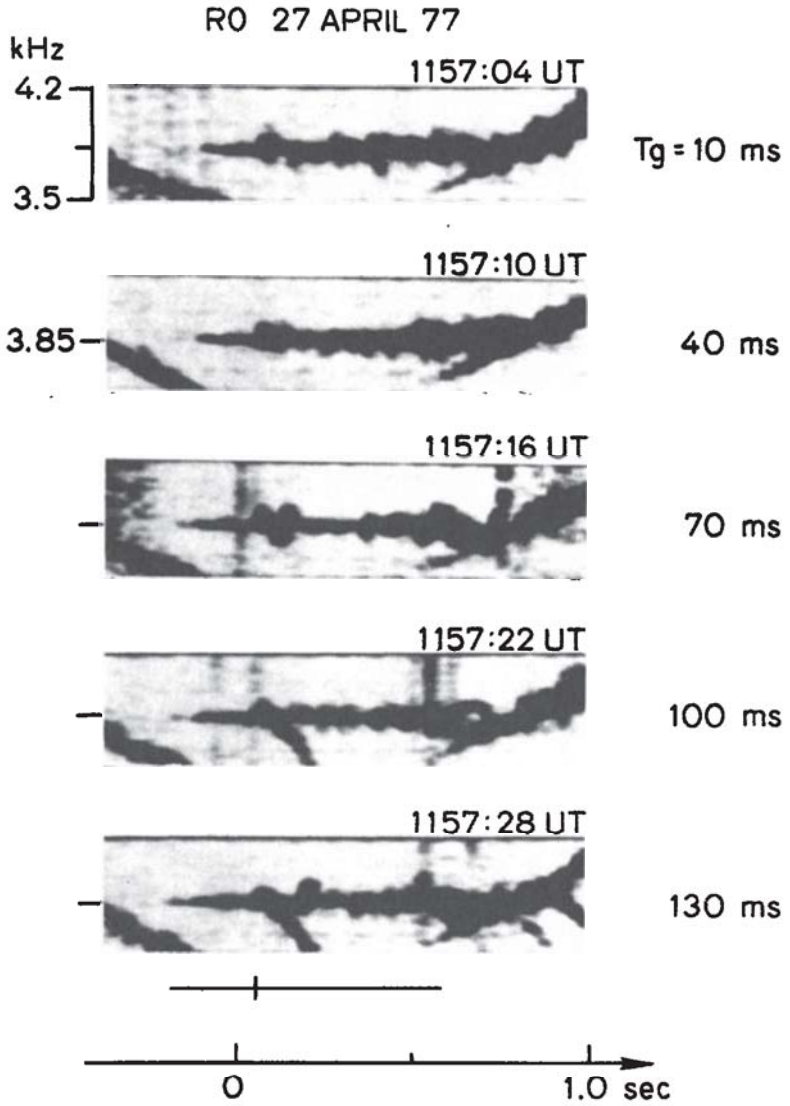

Figure 4. The features of gap-induced emissions versus various gap sizes.

by fully developed falling and/or rising emissions. But the pregap sections (200 or 400 ms long) of the gap-triggering pulses trigger BLI-type emissions only. There are no fully developed falling or rising emissions following the BLIs, suggesting that the emissions are either suppressed or entrained by the postgap section rate of the applied signals. Remembering that the postgap growth rate of the applied signals is the same as the initial growth rate in all examples shown in Figure 2, we rule out the possibility of entrainment. Therefore we conclude that the emissions have been suppressed by the main signals and that the main signal following the gap has not been significantly altered by the emissions in this particular case.

Average values of initial growth rate, postgap growth rate, and the saturation level are listed in Table 1 for over 52 examples taken on April 28 and May 13, 1975. The result shows that the saturation levels and growth rates are practically the same for both the pregap and postgap sections of the pulse and are independent of whether the postgap signal is an 0 wave or a π wave.

The data from the 10-ms fixed-gap experiments show many instances of induced rising emissions coming from the gaps. So far, no fully developed falling emission has been observed within a 10-ms gap, indicating that falling emissions require a larger gap for their development. To investigate this question, an experiment was performed in which a gap of variable length was introduced into a constant-frequency pulse, as shown in Figure 4. Each pulse was 750 ms long, and the gap was started at the two hundred fiftieth millisecond. The gap length T_g was stepped through five different values: 10, 40, 70, 100, and 130 ms. The phase of the pulse remained unchanged after the gap. Using ramp signals (not shown), two dominant paths were found. The difference in travel time for these two paths at 3.85 kHz was about 50 ± 10 ms.

As the gap length T_g increased from 10 to 70 ms, all the gap-induced emissions on both paths were either suppressed or entrained by the postgap signals. When T_g equalled or exceeded 100 ms, a fully developed falling emission was observed on path 1 (shorter delay). On path 2, however, the emission was captured for all values of T_g. This is because the absolute slope $|df/dt|$ of the emission was smaller on path 2. At the end of the 70-ms gap the emission frequency on path 1 was approximately the same as that of the applied signal. During capture by the postgap signal the emission continued to fall in frequency to about 100 Hz below the carrier. At this point the natural emission had become suppressed, and all phase-bunched currents appeared to come under the control of the applied wave. The details of this process are under study and will be reported in a later paper.

Acknowledgements. We thank our colleagues, T. F. Bell, D. L. Carpenter, and C. G. Park, for helpful comments on the manuscript. We also thank J. P. Katsufrakis for his effective management of the field stations employed in these experiments and thank K. Dean and G. Daniels for preparation of the typescript. This work was supported in part by the Division of Polar Programs of the National Science Foundation under grant DPP76-82646 and the Atmospheric Sciences Section of the National Science Foundation under grant ATM78-05746.

The Editor thanks M. J. Rycroft and another referee for their assistance in evaluating this paper.

References

Bell, T. F., ULF wave generation through particle precipitation induced by VLF transmitters, J. Geophys. Res., 81, 3316, 1976.

Brice, N., Fundamentals of VLF emission generation mechanisms, J. Geophys. Res., 69, 4515, 1964.

Chang, D. C. D., VLF wave-wave interaction experiments in the magnetosphere, Ph.D. thesis, Radiosci. Lab. Tech. Rept. 3458-1, Stanford Univ., Stanford, Calif., May 1978.

Dowden, R. L., A. D. McKay, L. E. S. Amon, H. C. Koons, and M. H. Dazey, Linear and nonlinear amplification in the magnetosphere during a 6.6-kHz transmission, J. Geophys. Res., 83, 169, 1978.

Helliwell, R. A., A theory of discrete VLF emissions from the magnetosphere, J. Geophys. Res., 72, 4773, 1967.

Helliwell, R. A., Wave-wave interactions in the magnetosphere, paper presented at the General Assembly, Union Radio Sci. Int., Helsinki, 1978.

Helliwell, R. A., and T. L. Crystal, A feedback model of cyclotron interaction between whistler-mode waves and energetic electrons in the magnetosphere, J. Geophys. Res., 78, 7357, 1973.

Helliwell, R. A., and J. P. Katsufrakis, VLF wave injection into the magnetosphere from Siple Station, Antarctica, J. Geophys. Res., 79, 2511, 1974.

Helliwell, R. A., J. P. Katsufrakis, and M. L. Trimpi, Whistler-induced amplitude perturbation in VLF propagation, J. Geophys. Res., 78, 4679, 1973.

Helliwell, R. A., J. P. Katsufrakis, T. F. Bell, and R. Raghuram, VLF line radiation in the earth's magnetosphere and its association with power line radiation, J. Geophys. Res., 80, 4247, 1975.

Ho, D., and L. C. Bernard, A fast method to determine the nose frequency and minimum group delay for a whistler when the causative spheric is unknown, J. Atmos. Terr. Phys., 35, 881, 1973.

Koons, H. C., M. H. Dazey, R. L. Dowden, and L. E. S. Amon, A controlled VLF phase reversal experiment in the magnetosphere, J. Geophys. Res., 81, 5536, 1976.

McPherson, D. A., H. C. Koons, M. H. Dazey, R. L. Dowden, L. E. S. Amon, and N. R. Thomson, Conjugate magnetospheric transmissions at VLF from Alaska to New Zealand, J. Geophys. Res., 79, 1555, 1974.

Nunn, D., A self-consistent theory of triggered VLF emissions, Planet. Space Sci., 22, 349, 1974.

Raghuram, R., T. F. Bell, R. A. Helliwell, and J. P. Katsufrakis, Echo-induced suppression

of coherent VLF transmitter signals in the magnetosphere, J. Geophys. Res., 82, 2787, 1977a.

Raghuram, R., T. F. Bell, R. A. Helliwell, and J. P. Katsufrakis, A quiet band produced by VLF transmitter signals in the magnetosphere, Geophys. Res. Lett., 4, 199, 1977b.

Rosenberg, T. J., R. A. Helliwell, and J. P. Katsufrakis, Electron precipitation associated with discrete VLF emissions, J. Geophys. Res., 76, 8445, 1971.

Smith, R. L., and D. L. Carpenter, Extension of nose whistler analysis, J. Geophys. Res., 66 2583, 1961.

Stiles, G., and R. A. Helliwell, Stimulated growth of coherent VLF waves in the magnetosphere, J. Geophys. Res., 82, 523, 1977.

(Received August 17, 1978;
revised September 14, 1979;
accepted September 18, 1979.)